

Recovery after Mode I crack propagation and impact in E-glass reinforced Poly(ϵ -caprolactone)/epoxy blends

Amaël Cohades¹, Véronique Michaud²

Laboratoire de Technologie des Composites et Polymères (LTC), Institute of Materials, Ecole Polytechnique Fédérale de Lausanne (EPFL), CH-1015 Lausanne, Switzerland

¹ E-mail: amael.cohades@epfl.ch, Web Page: <http://www.ltc.epfl.ch>

² E-mail: veronique.michaud@epfl.ch, Web Page: <http://www.ltc.epfl.ch>

Keywords: self-healing materials, fiber reinforced polymers, polycaprolactone, interlaminar fracture toughness, impact testing

Abstract. Blends of commercial epoxy monomer with a 4,4'-diaminodiphenylsulfone hardener and poly(ϵ -caprolactone) (PCL) were used as a matrix in woven glass fiber-reinforced polymer composites (FRPs). FRPs with these blends (containing 0, 25 and 37vol% of PCL) were manufactured through Vacuum Assisted Resin Infusion Molding. The blends morphology resulting from polymerization induced phase separation consisted of interconnected epoxy particles embedded in a PCL matrix. Morphological development was prevented within the fiber tows when the expected structure was coarser than the mean inter-fiber distance. Composites storage modulus at room temperature remained similar, however toughness decreased by 35% (from 950 to 620 J/m²) in the blend matrix composite with 25vol% PCL. Up to 50% toughness recovery was observed over multiple cycles when the blend composites were re-tested after Mode I DCB crack propagation followed by a thermal cycle at 150°C for 30 minutes. Comparison of impact properties showed lower performance for blend matrices as compared to plain composites. Healing efficiencies in terms of ultimate compressive residual strength and damage area recovery were 9.9 and 34% respectively, as a large damage extent resulted from the impact. The blend matrix composites therefore showed an ability to partially recover mechanical properties after matrix microcracking, but remained sensitive to large damage extent.

1. Introduction

Considerable effort has been made over the last 25 years to integrate self-healing functionality into thermoset polymers for the autonomous repair of sub-critical damage. Many current approaches to self-healing are based on incorporation of capsules or vascular systems that release a healing agent in the presence of a crack. The healing agent may be a reactive monomer that polymerizes on contact with a catalyst present in the polymer, for example, thus healing the crack, or a solvent capable of activating residual reactive groups within the polymer itself [1]. An alternative strategy is to prepare a miscible [2] or immiscible [3], [4] blend between the thermoset and a low melting point semicrystalline thermoplastic. For immiscible blends in particular, healing involves different concurrent mechanisms, whose effectiveness requires damage to propagate through the thermoplastic phase or along the interface between the thermoplastic and the thermoset: (i) melting and consequent volume expansion of the thermoplastic; (ii) flow of the thermoplastic melt into the damage zone; (iii) physical or chemical healing at the molecular level. The precise nature of the healing mechanism depends on the system and may involve either thermally activated re-establishment of entanglements across the crack faces or the re-establishment of reversible non-covalent bonds. This type of healing is repeatable as it implies the recovery of thermodynamic equilibrium in the thermoplastic phase.

In the study of Luo *et al.* [5] and our previous study [3], immiscible blends of commercial epoxy monomer with a 4,4'-diaminodiphenylsulfone (DDS) hardener and poly(ϵ -caprolactone) (PCL) were evaluated for their potential as a self-healing matrix for fiber-reinforced composites (FRPs), based on

toughness, stiffness and their capacity for healing when subjected to a moderate heating cycle. Analysis of the microstructure and thermal properties of the blends indicated three types of morphology to result from polymerization-induced phase separation during cure, depending on the PCL content, including an interconnected particulate epoxy phase and a co-continuous PCL phase above 23vol% PCL. While the mechanical performance diminished with increasing PCL content, toughness recovery after healing at 150 °C for 30 min strongly increased. Blends with 25vol% PCL showed a healing efficiency higher than 70 %, while retaining suitable room-temperature mechanical properties, and were concluded to be promising candidates for self-healing composites.

In the present study we investigated the use of epoxy-PCL blends as a matrix for FRPs. In particular, we manufactured FRPs with these blends (as well as with pure epoxy for comparison) through Vacuum Assisted Resin Infusion Molding (VARIM) at high temperature. Thermal and morphological properties, interlaminar properties as well as resistance to impact and compression after impact (CAI) were assessed on the produced composites. These samples were then used to investigate the self-healing capacity of the blends after damage and subsequent healing at 150 °C for 30 minutes.

2. Materials and methods

2.1. Materials and processing

EponTM 828EL (Momentive) was blended with different amounts of PCL ($M_n \approx 45,000$ g/mol, *Sigma Aldrich* for Mode I DCB tests; or $M_n \approx 50,000$ g/mol, *Perstorp* for impact and CAI tests) and then cured with DDS (DDS 98 %, *ABCR*, 2:1 molar ratio with respect to the epoxy). The different amounts of PCL initially mixed with the epoxy monomer are given in Table 1 as the mass ratios of the two components ($m_{\text{epoxy}}:m_{\text{PCL}}$), and the volume fractions of PCL determined after addition of the DDS, ϕ_{PCL} . These blends were then used for composite production. The used glass fiber reinforcement (*Suter-Kunststoffe AG*) was a woven twill 2x2 E-glass fabric, with a nominal areal weight of 390 g/m². The resulting fiber volume fractions within each composite are also given in Table 1.

Table 1: Specimen designations, mass ratios of epoxy resin to PCL, overall PCL volume fractions after addition of the DDS and fiber volume fraction obtained after composite production.

Specimen	epoxy to PCL	PCL volume fraction in matrix	Fiber volume fraction in sample
	$m_{\text{epoxy}}:m_{\text{PCL}}$	ϕ_{PCL}	V_f
Plain	100:0	0	48.6±1.8
PCL(25)	72:28	25.0	48.8±0.7
PCL(37)	59.5:40.5	36.9	47.5±1.9

The three types of composite plates were processed by VARIM. Sixteen layers of fiber reinforcement were cut in 210x180 mm rectangles and stacked with a sequence of $[(+45/-45)/(0/90)]_{4s}$. A target fiber volume fraction (V_f) of 50 vol% and a final plate thickness of 5 mm were sought. A release film (*Cytec*, 15 μm , non-perforated) was placed between the two central plies to form the notch which was the starting point for the delamination in Mode I (DCB) samples. The used lay-out design was similar to that presented in [6] for successful production of DCB test samples. For impact test samples, plates with dimensions 250x350 mm and the same stacking sequence as for DCB Mode I were produced, without any notch on the central plies. Blends of PCL and epoxy were prepared with the compositions indicated in Table 1 following a similar procedure to that of Luo *et al.* [5] and our previous study [3]. These blends were then infused through the reinforcement at a temperature of 140°C, ensuring a viscosity below 1 Pa·s. The plate underwent a curing treatment at 180°C for 3h, to reach full resin polymerization [3].

2.2. Morphological and thermomechanical characterization

Transverse cuts of the composite specimen were embedded in *Epofix* Resin, then polished until 1 μm size diamond disc polishing, and observed with a reflection optical microscopy (*Olympus* BH-2). Fracture surface of the DCB specimens, coated with 10 nm of gold, were also observed by scanning electron microscopy (SEM, *Philips* XLF-30 FEG).

Differential scanning calorimetry (DSC, TA Q100, TA Instruments): 5-10 mg samples from the cured composite specimens were subjected to heating scans from -90 to 300 $^{\circ}\text{C}$ at 10 $^{\circ}\text{C}/\text{min}$ followed by cooling to 0 $^{\circ}\text{C}$ at the same rate. **Dynamic mechanical analysis (DMA, TA Q800, TA Instruments):** 35 \times 12.5 mm^2 rectangles were cut from the composite specimens and tested at 1 Hz in single-cantilever mode, with a displacement amplitude of 15 μm . The temperature was ramped from -150 to 300 $^{\circ}\text{C}$ at 6 $^{\circ}\text{C}/\text{min}$.

2.3. Mode I Double Cantilever Beam Testing

The fracture behavior of the prepared samples was assessed in Mode I Double Cantilever Beam (DCB) following the ASTM D5528. Each sample underwent four loading-unloading cycles, the first one corresponded to the test of the *virgin* specimen, whereas the three others applied to the *healed* specimens after a thermal mending cycle of 30 minutes at 150 $^{\circ}\text{C}$. At least 7 tests were performed for each batch. During thermal mending, samples were left as unloaded, with only the crack faces imposed to be in contact on the loading blocks, leading to a maximum crack thickness of 100 μm . Steady-state interlaminar fracture toughness, G_{IC} , was calculated based on crack length measurements (Modified Beam Theory) and healing efficiency was further defined as:

$$\eta = \frac{G_{IC, \text{healed}}}{G_{IC, \text{virgin}}} \quad (1)$$

2.4. Impact testing and Compression After Impact properties

The impact behavior of the produced samples was assessed following the ASTM D7136 with a *Rosand* impact testing machine. The load imparted by the 5.5 Kg impactor was recorder by a *Kistler* load cell of 60 kN. At least 5 samples were tested for each batch (Plain and PCL(25) here only).

The compressive residual strength properties of the impacted samples were then assessed following the ASTM D7137 with a 600 kN *Schenk* universal testing machine. At least 3 samples were tested for each batch. Plain and PCL(25) samples were tested before (*virgin*) and after impact (*impacted*), and after healing (*healed*) at 150 $^{\circ}\text{C}$ for 30 minutes. Healing efficiency was defined as:

$$\eta = \frac{F_{CAI, \text{healed}} - F_{CAI, \text{impacted}}}{F_{CAI, \text{virgin}} - F_{CAI, \text{impacted}}} \quad (2)$$

The damage area in each impacted sample was quantified through C-scan tests. Each sample was protected with Teflon tape (to prevent water penetration), placed in a water bath and scanned with a 2.5 MHz piezoelectric transducer at steps of 0.2 mm. 2D-maps of the sample were generated and showed variation in the sound wave attenuation when damage is present.

3. Results and Discussion

3.1. Microstructural development in the blends

Optical microscopy images for transverse cuts of the cured samples are shown on Fig. 1 for Plain, PCL(25) and PCL(37) samples. The quality of the composite through the VARIM process is satisfactory: no porosity was observed (notice that the black regions around the composites with epoxy-PCL blends (Fig. 1 (b) and (c)) were due to polishing and the differences in strength existing inside this kind of material, removing the softer PCL regions). For *PCL(25)* sample (Fig. 1 (b)), the matrix two phase structure was found only in large spaces, i.e. in between the plies in the resin rich regions. Therefore, in this kind of FRPs, phase separation was prevented within the fiber tows, making the structure to be different between (phase separated) and within (continuous epoxy phase) tows. This observation can be related to the measurement of epoxy particle diameters in resin rich areas, which were $17.12 \pm 2.66 \mu\text{m}$ in the resin rich region, higher than the distance between two fibers within a tow. In addition, these measured diameters were slightly smaller than measured previously in bulk resin systems ($20.14 \pm 4.75 \mu\text{m}$) [3], which indicated that phase separation was delayed by the presence of fibers. For *PCL(37)* sample (Fig. 1 (c)), however, phase separation could be observed between and within tows of the composite. As epoxy particle diameters were of $3.55 \pm 1.05 \mu\text{m}$, particles could fit between fibers within tows. Notice again that these measured diameters were slightly smaller than observed in neat resin systems ($7.36 \pm 1.58 \mu\text{m}$) [3]. Even though phase separation was present within tows of *PCL(37)* sample, a continuous epoxy layer could be observed around the glass fibers, which can be explained by preferential wetting of the epoxy as compared to PCL [7].

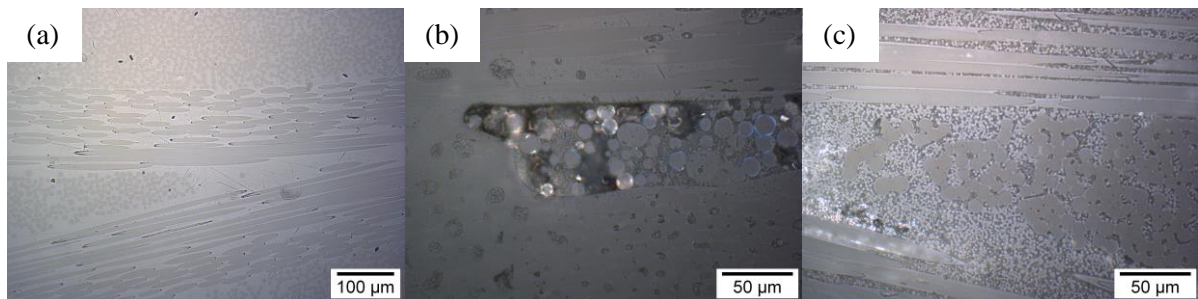


Figure 1: Transverse cut of the three assessed samples: (a) *Plain*; (b) *PCL(25)*; (c) *PCL(37)*.

3.2. Thermomechanical properties

Fig. 2 (a) shows DSC heating scans for the three different samples after cure. Two characteristic transitions were observed for all the compositions. The endothermic peak at about 54 °C corresponded to melting of the PCL, whereas the small enthalpy peak at about 197 °C was associated with the glass transition of the epoxy. These transition temperatures were generally similar to those of the pure PCL and pure epoxy, indicating a high degree of phase purity. Notice also that no exothermic peak can be observed on these heating scans, indicating that the obtained composite was in its fully cured state and that the presence of fibers did not influence the required matrix curing schedules [3].

Thermomechanical properties were then determined by DMA. The storage modulus, E' , is shown as a function of PCL content in Fig. 2 (b) for two relevant temperatures, 25 °C (room temperature) and 150 °C (the target healing temperature). At room temperature, a decrease in E' from 6.6 to close to 6.3 GPa was observed as the PCL content increased from 0 to 25vol% in the matrix, indicating a nearly constant modulus between those two compositions thanks to the interconnectivity of the epoxy particles. Further increasing the PCL content (to 37vol% in the matrix) led however to a larger

modulus decrease, down to 4.6 GPa, mainly due to the higher PCL content, which decreased the particle size and interconnectivity [3]. At 150 °C, E' decreased from about 5.5 GPa for the plain sample to about 3.7 GPa for $PCL(25)$ sample and about 1.5 GPa for $PCL(37)$ sample, reflecting the molten state of the PCL. However, even at 150 °C, this blend behaved globally as a stiff elastic solid, and no significant dimensional instabilities were observed, indicating the contacts between the epoxy particles to be sufficient to maintain structural integrity at the healing temperature.

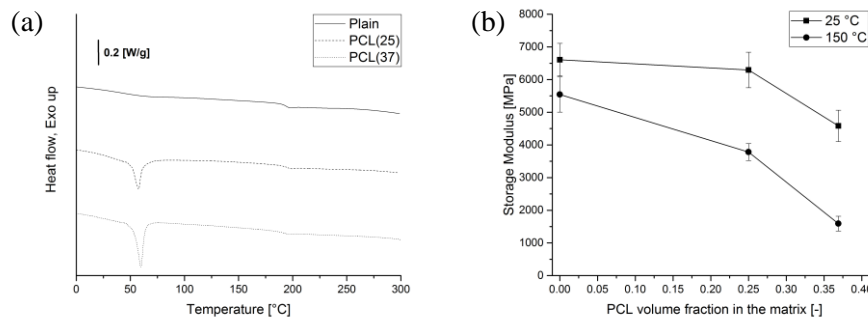


Figure 2: (a) DSC heating scans for the different samples after cure.; (b) E' determined by DMA as a function of the PCL V_f in the matrix at room temperature and the healing temperature (150 °C).

3.3. Mode I Double Cantilever Beam Testing

Fig. 3 (a) shows fracture toughness mean values for both the plain and epoxy-PCL composites. Notice first that the value obtained for the plain system (950 J/m²) was similar to what was measured in previous studies [6]. As compared to the plain system, a decrease of 35% and 55% in fracture toughness was observed for respectively $PCL(25)$ and $PCL(37)$ samples. This decrease could be explained by the intrinsic behavior in fracture toughness of the blends where the PCL exists as a confined layer in between the epoxy particles, as determined in our previous study [3]. Even though each glass fiber of the composite was surrounded by a layer of pure epoxy, toughness was reduced for $PCL(25)$ and $PCL(37)$ samples due to the surrounding softer environment of the blends. Notice that in a composition range between 0 and 25% PCL, toughness could go through a maximum due to the resulting phase separation morphology (PCL particles in epoxy matrix) [8]. Multiple healing efficiencies were determined in terms of toughness, based on Eq. (1) and are shown for $PCL(25)$ and $PCL(37)$ on Fig. 3 (b) for three healing cycles. Efficiencies for Plain samples are not depicted as their value was null, as expected. Both $PCL(25)$ and $PCL(37)$ exhibited moderate recovery in toughness after thermal mending. Notice first that the scatter was relatively high due to the difficulty in properly determining the advancement of the crack in the healed state (the thermoplastic often did not wet the entire sample surface). Recovery in properties was higher for higher PCL contents and an increasing number of healing cycles, which could be explained by the higher expansion and spatial distribution of the PCL in the crack after several healing cycles. Incomplete recovery in fracture toughness has been explained by incomplete crack filling during healing of the samples as those were not clamped during healing. From the study of Rodgers [9], it was possible to measure the PCL expansion capacity at healing temperature (14% here), and therefore determine the maximum thickness that the PCL could fill considering the DCB geometry and PCL content. For the present case, the PCL had the ability to fill a crack of 36 μm (for a $PCL(37)$ sample, this value is 53 μm), which is lower than the 100 μm crack thickness observed in unloaded DCB samples.

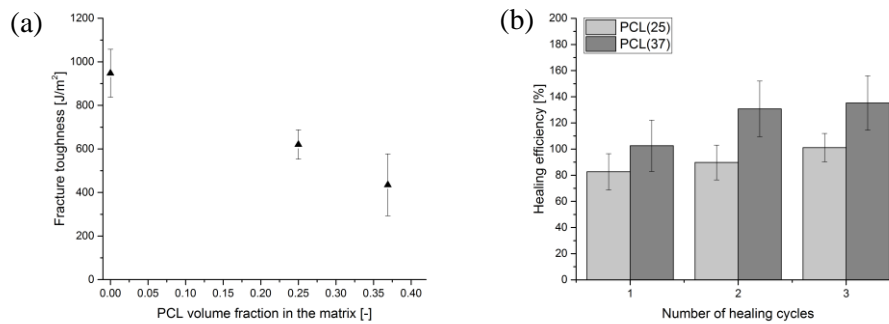


Figure 3: (a) Fracture toughness as a function of the PCL volume fraction in the matrix; (b) Multiple healing assessment in terms of toughness based calculation for PCL(25) and PCL(37).

Fig. 4 (a) shows a SEM image of the fracture surface for *PCL(25)* specimen after a virgin testing cycle indicating that failure was dominated by interfacial debonding between the fibers and the matrix as usually observed in woven composites [6]. The phase separated particulate morphology was well observed in the resin rich regions of the surface. Fig. 4 (b) depicts the fracture surface of *PCL(25)* specimen observed by SEM, after one healing cycle. Whereas interfacial debonding could be observed, as in the case after a virgin cycle (Fig. 4 (a)), the surface was now partially covered by PCL thanks to its expansion and bleeding within the crack. After healing, a new interphase was therefore created between the fibers and PCL (as compared to fibers with epoxy during the virgin cycle), which explained recovery in fracture properties. Observation of the fracture surface for the same sample after multiple healing cycles showed higher amount of PCL coverage, explaining the higher efficiencies.

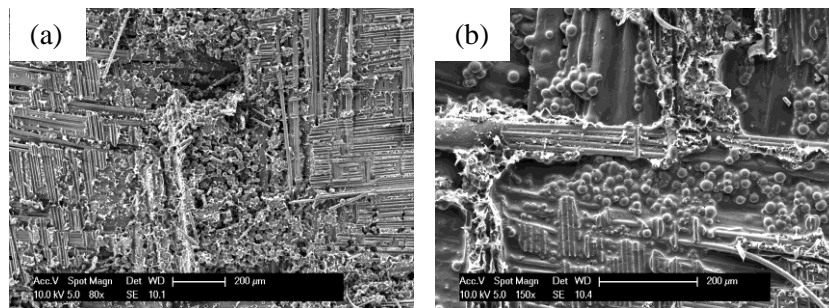


Figure 4: SEM image of a DCB fracture surface for *PCL(25)* specimen after (a) a virgin cycle and (b) one healing cycle.

3.4. Impact and Compression After Impact (CAI) properties

Impact and CAI properties were quantified here only for Plain and PCL(25) samples. The dissipated energy after an impact event (Fig. 5 (a)) was higher for PCL(25) (by 16%) as compared to Plain samples, which was directly linked to the lower strength previously observed for epoxy-PCL blends [3]. The ultimate residual compressive strength (F_{CAI}) was then quantified for non-impacted as well as impacted samples (Fig. 5 (b)). Again, F_{CAI} for non-impacted PCL(25) samples was lower (by 34%) as compared to Plain samples due to the lower matrix strength. Because the observed dissipated energy for epoxy-PCL composites was higher than for Plain samples, F_{CAI} for PCL(25) impacted samples was also lower (35%) as compared to pure epoxy composites. Thermal mending at 150°C for 30 minutes was performed on some PCL(25) impacted samples prior to CAI test and revealed a slightly higher residual strength as compared to non-healed samples thanks to PCL ability to flow within the crack.

Healing efficiency for this case was quite low (9.9%), but the part was severely damaged with 30 Joules energy following ASTM D7136. Therefore, cracks higher than 36 μm have been most probably induced and not healed during healing. Also, a non-negligible part of the damage event consisted of fiber breakage (fibers that could not be healed) due to the high impact energy, which considerably lowered the healing efficiency that could be reached. The damage area of the impacted samples has been further assessed through C-scan analysis. Those revealed a damaged area of 416 mm^2 for Plain samples and of 1598 mm^2 for PCL(25) samples therefore confirming the behavior observed during CAI tests. Filling of the damaged for PCL(25) could also be quantified (Fig. 6 for C-scan before and after healing) and demonstrated that the damaged area decreased by $34\% \pm 6.6\%$. Incomplete filling is again not surprising due to the large damage amount imparted to the samples. Even though recovery of properties after impact did not demonstrate high efficiencies, impacts with lower energy would affect only the FRPs matrix and could thus be more representative of microcracks healing targeted here.

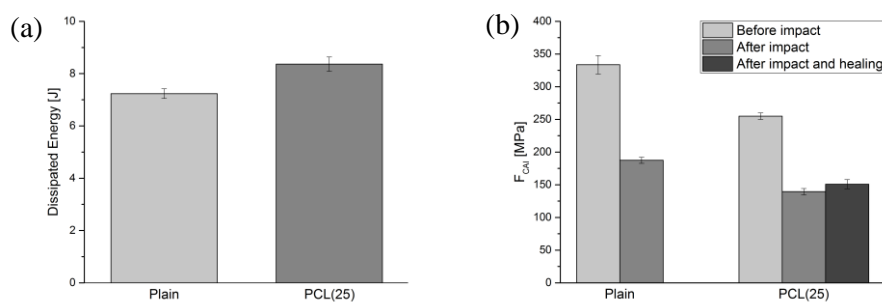


Figure 5: (a) Dissipated energy after impact for Plain and PCL(25); (b) ultimate compressive residual stress, F_{CAI} , before and after impact as well as after healing for PCL(25).

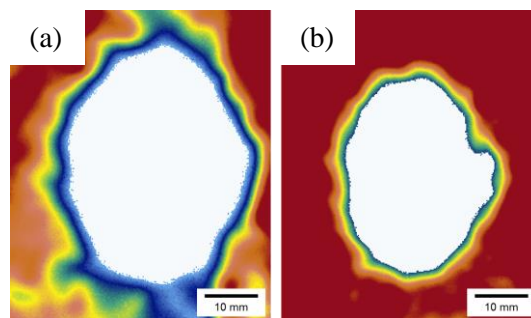


Figure 6: C-scan of an impacted PCL(25) sample (a) before healing; (b) after healing. Colors represent sound speed variation except white that shows complete absorption in the crack.

4. Conclusion

Glass fiber reinforced epoxy-PCL plates with fiber volume fractions of 50vol% could be processed through VARIM at elevated temperature. Microstructure observations of the composite with epoxy-PCL blends demonstrated the influence of the fiber reinforcement on the phase separation process. Indeed, phase separation and development of the epoxy particulate morphology could happen only in the resin rich regions of the reinforcement due to space constraint. This space constraint was observed as less critical for higher PCL contents as the diameters of the epoxy particles were smaller, which allowed particles to be inserted within fiber tows. Assessment of mechanical properties of these blends modified composites as compared to plain composites did not show significant influence in storage moduli whereas Mode I DCB testing did show considerable decrease in toughness when PCL was

added to the system due to the lower intrinsic fracture toughness of epoxy-PCL blends. Mode I testing further allowed the determination of toughness healing efficiencies over several cycles. For both composites modified by PCL, higher efficiencies were observed for higher PCL content as well as when increasing the number of healing cycles and could reach 50% recovery thanks to the PCL ability to bleed and expand within the crack. Comparison of impact and CAI properties showed again lower values for epoxy-PCL matrices as compared to plain composites. Healing efficiencies in terms of ultimate compressive residual stress and damage area recovery were of 9.9 and 34% respectively, the large damage amount as well as fiber breakage imparted to the samples being the main cause for those low efficiencies. Providing lower damage amount to the part in order to quantify healing efficiency for only matrix microcracking needs thus further assessment. Even though phase separation was affected by the presence of fibers in FRPs, it can be concluded from the present findings that 25vol% of PCL within the matrix should give suitable healing efficiencies for matrix microcracking recovery (in terms of toughness and impact recovery) in FRPs without any deterioration in modulus of the composite.

5. Acknowledgments

This work is funded by the Swiss National Science Foundation (SNF 200020-150007-1). We would like to thank Perstorp for providing the PCL, the Interdisciplinary Centre of Electron Microscopy (CIME) for SEM imaging, COMATEC institute at HEIG-VD for C-scan tests, the Laboratory of Mechanical Metallurgy (LMM) for CAI tests and G. Riesen for his technical assistance.

6. References

- [1] B. J. Blaiszik, S. L. B. Kramer, S. C. Olugebefola, J. S. Moore, N. R. Sottos, and S. R. White, "Self-Healing Polymers and Composites," *Annu. Rev. Mater. Res.*, vol. 40, no. 1, pp. 179–211, Jun. 2010.
- [2] S. a Hayes, W. Zhang, M. Branthwaite, and F. R. Jones, "Self-healing of damage in fibre-reinforced polymer-matrix composites.," *J. R. Soc. Interface*, vol. 4, no. 13, pp. 381–387, Apr. 2007.
- [3] A. Cohades, E. Manfredi, J.-C. Plummer, and V. Michaud, "Thermal mending in phase-separated Poly(ϵ -caprolactone)/epoxy blends-SUBMITTED," *Eur. Polym. J.*, 2016.
- [4] S. Meure, R. J. Varley, D. Y. Wu, S. Mayo, K. Nairn, and S. Furman, "Confirmation of the healing mechanism in a mendable EMAA-epoxy resin," *Eur. Polym. J.*, vol. 48, no. 3, pp. 524–531, 2012.
- [5] X. Luo, R. Ou, D. E. Eberly, A. Singhal, W. Viratyaporn, and P. T. Mather, "A thermoplastic/thermoset blend exhibiting thermal mending and reversible adhesion," *ACS Appl. Mater. Interfaces*, vol. 1, no. 3, pp. 612–20, Mar. 2009.
- [6] E. Manfredi, A. Cohades, I. Richard, and V. Michaud, "Assessment of solvent capsule-based self-healing for woven E-glass fibre-reinforced polymers," *Smart Mater. Struct.*, vol. 24, pp. 1–11, 2015.
- [7] D. J.-P. Turmel and I. K. Partridge, "Heterogeneous phase separation around fibres in epoxy/PEI blends and its effect on composite delamination resistance," *Compos. Sci. Technol.*, vol. 57, pp. 1001–1007, 1996.
- [8] K. P. Unnikrishnan and E. T. Thachil, "Toughening of epoxy resins," *Des. Monomers Polym.*, vol. 9, no. 2, pp. 129–152, Mar. 2012.
- [9] P. A. Rodgers, "Pressure-Volume-Temperature Relationships for Polymeric Liquids: A review of Equations of State and Their Characteristic Parameters for 56 Polymers," *J. Appl. Polym. Sci.*, vol. 48, no. 6, pp. 1031–1080, 1993.